

# Optical Sigma-Delta Modulation Using Fiber Lattice Filter Structures

P. E. Pace, S. J. Ying, J. P. Powers, and R. J. Pieper  
*Department of Electrical and Computer Engineering  
Naval Postgraduate School, Monterey, California 93943*

## Abstract

Modern avionics equipment, such as super resolution direction-finding systems, now require resolutions on the order of 20 to 22 bits. Oversampled analog-to-digital converter architectures offer a means of exchanging resolution in time for that in amplitude and represent an attractive approach to implementing precision converters without the need for complex precision analog circuits. Using oversampling techniques based on sigma-delta ( $\Sigma\Delta$ ) modulation, a convenient tradeoff exists between sampling rate and resolution. One of the major advantages of integrated optics is the capability to efficiently couple wideband signals into the optical domain. Typically,  $\Sigma\Delta$  processors require simple and relatively low-precision analog components and thus are well suited to integrated optical implementations. This paper presents the design of a first-order, integrated optical  $\Sigma\Delta$  modulator.

## 1 Introduction

Analog-to-digital converters (ADCs) are basic building blocks for a wide variety of digital systems. A partial list of ADC applications includes process control, automatic test equipment, video signal acquisition, audio recordings for compact disc and interfaces for personal computers. There exists a variety of approaches to the ADC design. One approach, known as delta modulation, involves the use of oversampling methods. First introduced in the 1940s, delta modulation uses oversampling and single-bit code words to represent the analog signals [1]. The simplest approach counted the output bits from the delta modulator with a high bit representing a +1 and a low bit a -1. The output was then resampled at the Nyquist rate. Resolution proved to be a problem, since achieving adequate reproduction of speech signals required oversampling ratios on the order of 5,000. More effec-

tive digital filtering was needed to prevent the high-frequency modulation noise from aliasing into the signal band when it was resampled at the Nyquist rate.

Unfortunately at that time, digital filters used for this purpose were prohibitively expensive. Candy proposed an interpolative technique for digital filtering [2]. The idea was to digitize the signal through the use of a coarse quantizer and cause the output to oscillate between the quantized levels at high speed so that its average value over the Nyquist interval was an accurate representation of the sampled value. The digital filters used to generate this average were inexpensive. On the other hand, these digital filters also proved to be reliable and fairly tolerant of circuit imperfections. The quantizers for these interpolating converters utilized a noise-shaping technique which measures the quantization error in one sample and subtracts it from the next input sample value [3]. The most popular form of this noise-shaping technique is known as *sigma-delta modulation*. Sigma-delta modulators employ integration and feedback in iterative loops to obtain high-resolution A/D conversions.

Specifically, a sigma-delta modulator ( $\Sigma\Delta M$ ) consists of an analog filter and a quantizer enclosed in a feedback loop [4]. Together with the filter, the feedback loop acts to attenuate the quantization noise at low frequencies while amplifying the high-frequency noise. Since the signal is oversampled at many times the Nyquist rate, a digital low-pass filter may be used to remove the high-frequency quantization/modulation noise without affecting the signal band. This filtering usually involves a multi-stage decimation process since the output of the modulator represents the signal with the high-frequency modulation noise as well as its out-of-band components which dominate at the lower frequencies. In general, the smoothing characteristics involved in the decimation process require that the signal propagate through several filters and resampling stages. The first stage of decimation lowers the word rate to an intermediate

frequency, where a filter removes the high-frequency modulation noise. A second low-pass filter is then used to attenuate the out-of-band components before the signal is resampled at its Nyquist rate. As the signal propagates through the filters and resampling stages, the word length increases in order to preserve the resolution. A more thorough discussion of multi-stage decimation and filtering can be found in reference [1].

## 2 All Electronic, Single Bit, $\Sigma\Delta$ Modulation

A sampled-data equivalent of a first-order  $\Sigma\Delta$  is shown in Figure 1. Because this is a sampled-data circuit, the integration is performed via an accumulator. The analog signal is assumed to be oversampled at well above the Nyquist frequency. This sampled input,  $x_i$ , is fed to the quantizer via the accumulator. The quantized output, which can be modeled as an approximation of the quantization error, is fed back and subtracted from the input. This quantized, feedback signal forces the average value of the quantized output,  $y_i$ , to track the average value of the input signal. Any difference accumulates in the integrator and eventually corrects itself.

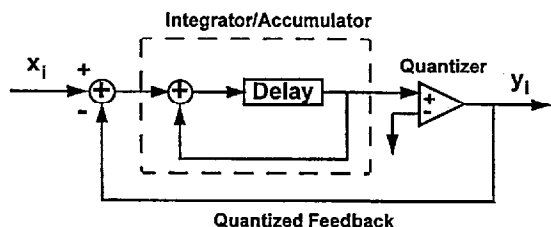


Figure 1: Block diagram of a 1st-order all-electronic  $\Sigma\Delta$ .

The quantization error is subtracted from the input value and the difference becomes the input for the next cycle. After the process is repeated many times at high speed, an average of the digital outputs occurring in each sample time becomes a useful digital representation of the input signal. In a stable converter, the oscillations of the quantized value are bounded, that is, it has a limit cycle. In general this quantization process can be performed over more than one quantization level [1]. By this process, it can be seen that the speed of operation obviates the need for precise circuit elements. Precision in the quantization levels of the quantizer is not a stringent requirement since the average of the quantized output,  $y_i$ , will automatically be adjusted to agree with the sampled input analog signal,  $x_i$ . Therefore the

output of the  $\Sigma\Delta$  modulation process can provide a high level of precision in the representation despite coarseness in the quantization levels.

The input/output transfer characteristics of the first-order  $\Sigma\Delta$  is plotted in Figure 2a. The signal oscillates between the quantized levels in such a manner that its local average equals the average input. For this example the input signal is ramped with 200 samples with a  $\pm 1$  volt range. The comparator output voltage is  $\pm 1$  volt with the threshold voltage set at zero volts. Figure 2b shows the limit cycles at the output of the accumulator. These simulation results are in agreement with previously reported predictions for first-order  $\Sigma\Delta$  modulators [1].

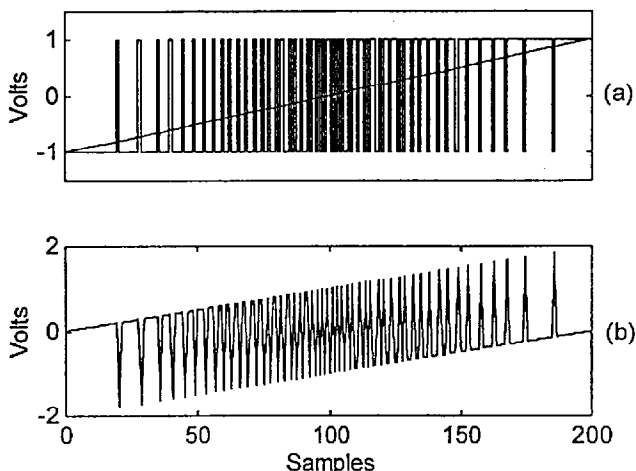


Figure 2: 1st-order all-electronic  $\Sigma\Delta$ . (a) Plot of comparator output and sampled input. (b) Plot of output of accumulator stage.

## 3 Integrated Optical, Single-Bit $\Sigma\Delta$ Modulator

A block diagram of a first-order, integrated optical  $\Sigma\Delta$  is shown in Figure 3. In applying optical integrated components to a  $\Sigma\Delta$  architecture, a first-order model is first simulated. In the integrated optical design, laser pulses from a mode-locked laser are used to oversample the RF signal. Mode-locked lasers are capable of providing a high pulse repetition frequency, narrow pulse widths and jitter times on the order of 200 fs. In order to gain a better understanding of the model, the integrated optical components used are described in detail.

### Mach-Zehnder Interferometer

A Mach-Zehnder interferometer (MZI) in a push-pull configuration is used to efficiently couple the wide-band RF signal into the optical domain. It also serves

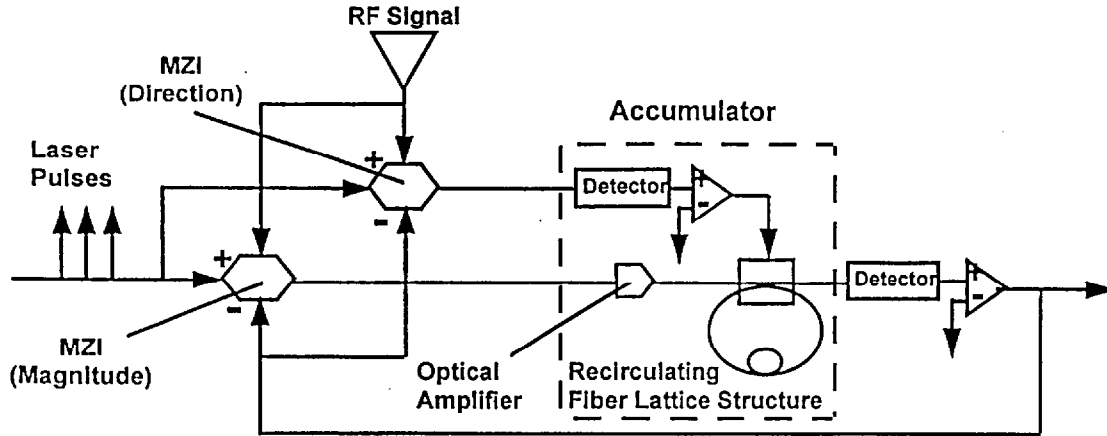


Figure 3: Block diagram of a 1st-order, integrated optical  $\Sigma\Delta M$ .

to subtract the feedback signal from the input signal. The configuration is utilized to subtract the feedback signal from the next input value. In order to take advantage of the push-pull MZI configuration, the feedback voltage polarity from the comparator must be reversed. The transfer function of the MZI [5] can be expressed as

$$I_{out} = I_{in} \left[ \frac{1}{2} + \frac{1}{2} \cos(\Delta\phi(\nu) + \theta) \right] \quad (1)$$

where

$$\Delta\phi(\nu) = \frac{2\pi n_e^3 r \Gamma L_i \nu}{G\lambda} \quad (2)$$

is the voltage-dependent phase shift and is a function of the effective index of the optical guide  $n_e$ , the pertinent electro-optic coefficient  $r$ , the interelectrode gap  $G$ , the electrical-optical overlap parameter  $\Gamma$ , and the free-space optical wavelength  $\lambda$ . The modulation voltage,  $\nu = V_{RF} - V_{FB}$ , serves to subtract the feedback signal from the next input value.

The method of accumulation involves the *magnitude* of the signal to be accumulated and the *direction* of accumulation. In the case of the first-order  $\Sigma\Delta M$ , two interferometers are used for the accumulator stage. One interferometer provides the *magnitude* for the accumulator. The other interferometer is used to determine the *direction* of accumulation. Figure 4 plots the transfer functions for both interferometers. Both MZIs map the input signal to an output intensity between zero and one (light intensity can not be negative). The transfer functions are the same except for the DC bias to induce a phase shift  $\theta$ . For the MZI controlling the magnitude of the signal,  $\theta = \pi$ . The MZI controlling the direction of accumulation has  $\theta = -\pi/2$ .

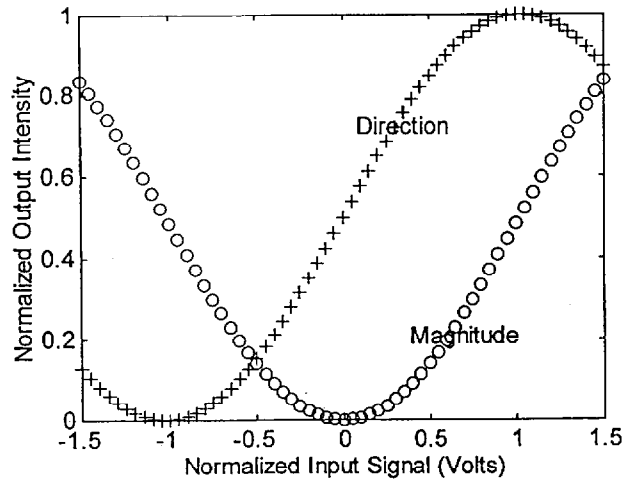


Figure 4: Transfer characteristic of the Mach-Zehnder interferometer.

As can be seen from the transfer functions, the output values for magnitude range from 0 to 0.5 and are symmetric about the input value of zero. The output values for the direction range from 0 to 1. The accumulator comparator threshold voltage is normalized at 0.5 volts. The detected *direction* intensity from the MZI is compared to the normalized threshold to determine whether the intensity from the *magnitude* MZI accumulates upward or downward. The recirculating fiber lattice structure accumulates downward if the output of the interferometer is less than 0.5 and upward for values greater than 0.5. Thus the detector, comparator and optical recirculator serve to function as an accumulator.

### Fiber Lattice Structures

Fiber-optic lattice structures incorporating single-mode fibers and directional couplers are used to in-

strument the accumulators. These fiber structures can be used to perform various frequency-domain functions such as matrix operations and frequency filtering [6]. Two structures basic to fiber signal processing include the two-coupler *nonrecirculating* and the two-coupler *recirculating* delay line. For design of the optical  $\Sigma\Delta$  modulator, a recirculating feedback fiber lattice structure is utilized for the accumulator. Moslehi, et al., described the z-transform transfer matrix of this recursive structure [6]. The inputs and outputs are related to each other by

$$\begin{pmatrix} Y_1(z) \\ Y_2(z) \end{pmatrix} = \begin{pmatrix} H_{11}(z) & H_{12}(z) \\ H_{21}(z) & H_{22}(z) \end{pmatrix} \begin{pmatrix} X_1(z) \\ X_2(z) \end{pmatrix}. \quad (3)$$

The transfer functions within the transfer matrix are

$$H_{11}(z) = \frac{a_1 - (1 - 2a_1)a_0L_1z^{-1}}{1 - a_1a_0L_1z^{-1}} \quad (4)$$

$$H_{21}(z) = \frac{1}{1 - a_0a_1L_1z^{-1}} \quad (5)$$

$$H_{12}(z) = \frac{\begin{pmatrix} 1 - 2a_0 - 2a_1 + 4a_0a_1 + a_0^2a_1^2 + a_0^2 \\ -2a_0^2a_1 + a_1^2 - 2a_1^2a_0 \end{pmatrix} L_1z^{-1}}{1 - a_0a_1L_1z^{-1}} \quad (6)$$

$$H_{22}(z) = \frac{-a_0 - a_1(1 - 2a_0)L_1z^{-1}}{1 - a_1a_0L_1z^{-1}} \quad (7)$$

and describe the use of the general structure where  $H_{mn}(z)$  is the transfer function from input  $X_n$  to output  $Y_m$ . Thus  $H_{21}(z)$  relates the  $X_1$  input and  $Y_2$  output and  $H_{12}(z)$  relates the  $X_2$  input and  $Y_1$  output. The parameters  $a_0$  and  $a_1$  are the intensity coupling coefficients of the directional couplers and  $L_1$  is the loop intensity transmittance of the system. For convenience  $L_1$  is assumed to be one (no losses in the system). The accumulator comparator voltage is then used to bias the directional coupler ( $a_1$ ) in order to create a phase change between the two pulses in order to perform the accumulation in the proper direction.

The accumulator stage in the first-order model has a transfer function given by

$$H(z) = \frac{Cz^{-1}}{1 - Dz^{-1}} \quad (8)$$

From the transfer matrix of the recirculating fiber lattice structure,  $H_{12}(z)$  matches this form where

$$\begin{aligned} C &= 1 - 2a_0 - 2a_1 + 4a_0a_1 + a_0^2a_1^2 \\ &\quad + a_0^2 - 2a_0^2a_1 + a_1^2 - 2a_1^2a_0 \end{aligned} \quad (9)$$

and

$$D = a_0a_1 \quad (10)$$

are the corresponding gain values. The specific lattice configuration is shown in Figure 5. The coupling coefficients  $a_0$  and  $a_1$  represent the percentage of light intensity coupled and therefore bounded between 0 and 1. The desired values for  $C$  and  $D$  would be unity. However, the two equations work against each other simultaneously as shown in Figure 6. Here  $a_0 = 0.3$  and  $a_1$  varies from 0 to 1. Values near the intersection of  $C$  and  $D$  provide the best results ( $a_1 = 0.5$ ,  $C = 0.122$ ,  $D = 0.15$ ). In order to compensate for the small value of  $C$ , an optical amplifier with a gain of 100 is placed just prior to the fiber lattice structure in the accumulator stage. Figure 7 plots the transfer characteristic of the first-order, integrated optical  $\Sigma\Delta$ .

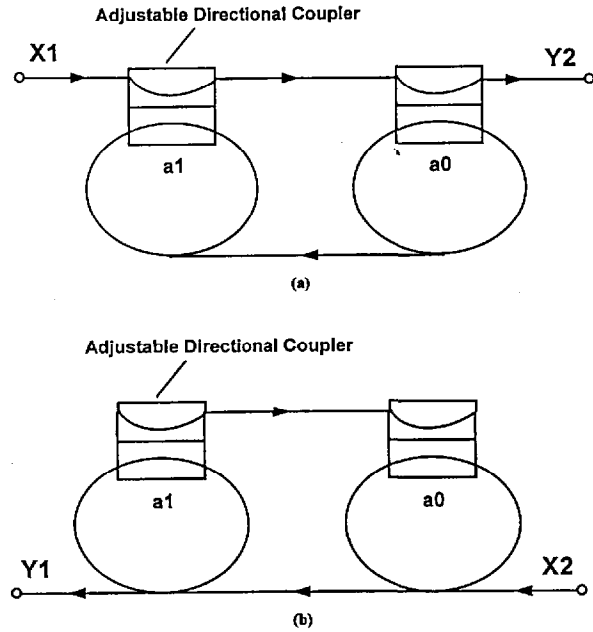


Figure 5: Block diagrams of specific fiber lattice configurations used for electro-optic  $\Sigma\Delta$ M. (a) First accumulator stage with transfer function  $H_{21}(z)$ . (b) Second accumulator stage with transfer function  $H_{12}(z)$ .

## 4 Conclusions

The  $\Sigma\Delta$  oversampling A/D modulator architecture uses limit cycles in quantized feedback loops to provide an accurate digital representation of the input signal. The use of fiber optic technology eliminates these limitations. An integrated optical first-order  $\Sigma\Delta$  architecture allows the processing of wideband RF signals. The integrated optical  $\Sigma\Delta$  design presented in this paper is a fairly straight-forward exten-

sion of the electronic design using standard integrated optical devices. Current simulation results confirm design feasibility.

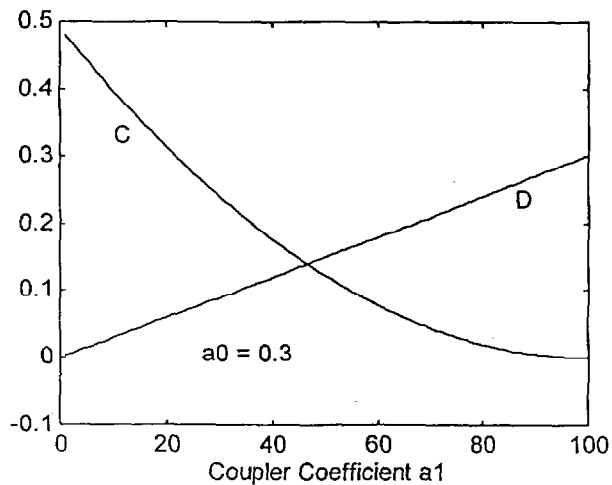


Figure 6: Plot of accumulator gains C and D as functions of  $a_0$  and  $a_1$ .

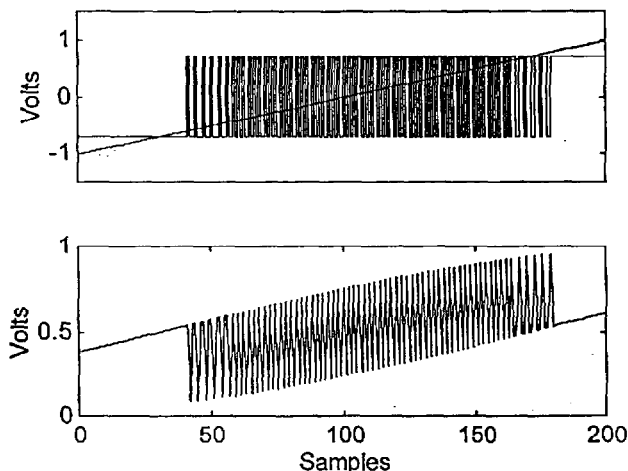


Figure 7: Transfer characteristic of 1st-order electro-optic  $\Sigma\Delta M$ .

## References

- [1] J.C. Candy and G.C. Temes, "Oversampling methods for A/D and D/A conversion," J.C. Candy and G.C. Temes, Eds., *Oversampling Delta-Sigma Data Converters*, IEEE Press, pp. 1-29, 1992.
- [2] J.C. Candy, "A use of limit cycle oscillations to obtain robust analog-to-digital converters," *IEEE Trans. Commun.*, Vol. COM-22, pp. 298-305, Mar. 1974.
- [3] C.C. Cutler, "Transmission systems employing quantization," 1960 U.S. Patent No. 2,927,962 (filed 1954).
- [4] B.E. Boser and B.A. Wooley, "The design of sigma-delta modulation analog-to-digital converters," *IEEE J. Solid-State Circuits*, Vol. 23, No. 6, pp. 1298-1308, Dec. 1988.
- [5] R.C. Alferness, "Waveguide electro-optic modulators," *IEEE Trans. Microwave Theory Tech.*, Vol. MTT-30, No. 8, pp. 1121-1137, Aug. 1982.
- [6] B. Moslehi, J.W. Goodman, M. Tur, and H.J. Shaw, "Fiber-optic lattice signal processing," *Proc. IEEE*, Vol. 72, No. 7, pp. 909-930, Jul. 1984.